

AGN and Star Formation in HerMES-IRS sources

Anna Feltre^{1,2}, Evanthia Hatziminaoglou²,
Antonio Hernán-Caballero³, Jacopo Fritz⁴ Alberto Franceschini¹
and HerMES

¹Dipartimento di Fisica e Astronomia, Università di Padova,
vicolo Osservatorio, 3, 35122 Padova, Italy

²ESO, Karl-Schwarzschild-Str. 2, 85748 Garching bei München, Germany

³Instituto de Fisica de Cantabria, CSIC-UC,
Avenida de los Castros s/n, 39005, Santander, Spain

⁴Sterrenkundig Observatorium, Vakgroep Fysica en Sterrenkunde Universeit,
Gent, Krijgslaan 281, S9 9000 Gent

Abstract. One of the remaining open issues in the context of the analysis of Active Galactic Nuclei (AGN) is the evidence that nuclear gravitational accretion is often accompanied by a concurrent starburst activity. We developed a spectral energy distribution (SED) fitting technique to derive simultaneously the physical properties of active galaxies and coexisting starbursts making the best use of *Spitzer* and *Herschel* IR observations. We apply the SED fitting procedure to a large sample of extragalactic sources representing the HerMES (*Herschel*/Multi-tiered Extragalactic Survey) population with IRS spectra with a plethora of multi-wavelength data in order to study the impact of a possible presence of an AGN on the host galaxy's properties. We analyze the star formation rate (SFR) in connection to the presence of an AGN and compared the properties of the hot (AGN) and cold (starburst) dust component. Our findings are consistent with no evidence for the presence of an AGN affecting the star formation processes of the host galaxies.

Keywords. galaxies: active – galaxies: starburst – galaxies: star formation – infrared: galaxies

1. Introduction

Intense episodes of star formation extend up to kpc scale, while in the inner tens pc of active galaxies we find, according with the unified model of AGN (Antonucci *et al.*, 1985; Urry *et al.*, 1995), a toroidal dusty structure surrounding the central super massive black hole. There is a lot of evidence for an intimate link between the two mechanisms both from the theoretical and observational side. Among the most important: i) the need to introduce AGN feedback to quench star formation in cosmological simulations and semi-analyticals models (e.g. Bower *et al.*, 2006; Croton *et al.*, 2006); ii) the correlation between the mass of the SMBH and that of the bulge of the host galaxy (e.g. Ferrarese & Merritt, 2000); iii) AGN and starbursts have been found to coexist in galaxies at all redshifts (e.g. Alexander *et al.*, 2005).

The main issue here is to understand whether a *causal* relationship exists between star formation and nuclear gravitational activity. Quantifying the relative importance between the two was, till recently, extremely difficult, as they both happen in dusty environment producing thus a lot of IR photons. It is exactly the IR where the efforts to investigate these two coeval phenomena should be concentrated. With data coming from *Spitzer* and *Herschel* we are now able to build the IR SED of extragalactic sources up to 500 μm . In particular, in the work presented here we use *Herschel*-SPIRE (250, 350 and 500 μm)

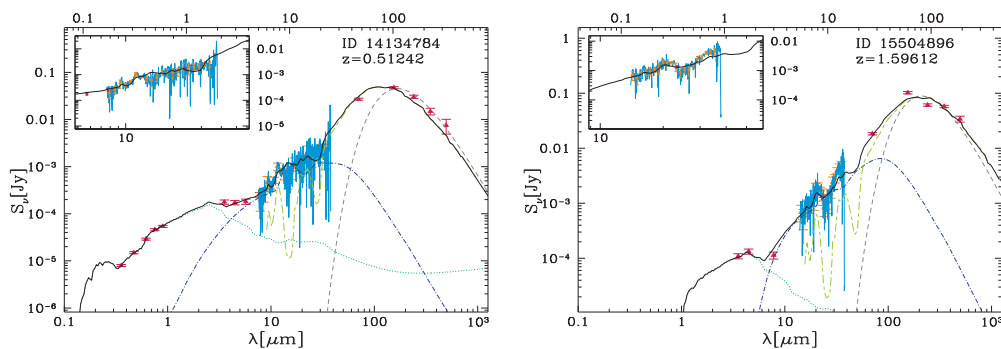


Figure 1. Examples of best-fitting to a low (left) and a high (right) redshift object (*Spitzer* ID 14134784 and 11867904, respectively). Three components of emissions are used to reproduce the IRS spectrum (turquoise; see also the insert figure) and photometric data (red symbols). The total model emission (black) is given by a combination of SSPs (dotted dark green line), AGN torus (dot dashed blue line) and starburst (dashed light green line). The black body emission, fitted at a second step, is shown in dashed gray. The top x-axis shows the rest-frame wavelength.

data coming from the HerMES (*Herschel* Multitired Extragalactic Survey, Oliver *et al.*, 2012) survey. These along with *Spitzer*-IRAC and -MIPS photometry allow us to cover both the peaks of the AGN (mid-IR) and starburst (far-IR) emissions. Moreover, the mid-IR spectra from the *Spitzer*-IRS spectrograph provide information about the emission and the absorption of the silicate features associated with the silicate grains in the dusty torus. PAH (Polycyclic Aromatic Hydrocarbons) molecules in star-forming regions also manifest themselves with spectral features between 6 and 13 μm . In this context the information coming from the IRS spectra plays a crucial role and the simultaneous use of *Spitzer* and *Herschel* data provide extensive information on the manner in which the two phenomena coexist.

2. Sample Description and SED fitting tool

Our sample comprises 375 sources with flux greater than 3σ at 250 μm , with σ comprising both the instrumental noise and the confusion limit (Roseboom *et al.*, 2010) in four of the northern HerMES fields, namely Bootes HerMES, FLS, Lockman Swire and ELAIS N1 SWIRE. All the sources of our sample had a reliable estimates of redshift (either from an optical or IRS spectrum) and IRS spectrum available from the Cornell Atlas of *Spitzer*/Infrared Spectrograph Project (CASSIS, Lebouteiller *et al.*, 2011).

To investigate simultaneously the properties of the AGN and starburst we applied a fully automatic multi-component SED fitting technique able to reproduce the optical/UV-to-FIR SED of galaxies. Three components of emissions are considered: i) a sum of simple stellar population models (SSP) having solar metallicity from Bertelli *et al.* (1994) to account for the stellar optical-UV emission, a revised grid of the Fritz *et al.* (2006) AGN torus models (presented in Feltre *et al.*, 2012) for the bulk of the mid-IR emission and empirical classical starburst templates to reproduce the emission at longer wavelengths. Photometric data and IRS spectra are fitted simultaneously with the methodology described in Feltre *et al.* (2013) in order to have more constraints on the models. In a second step, we fitted the photometric points at $\lambda > 100 \mu\text{m}$ with a modified black body (with the dust emissivity index kept fixed, $\beta = 2$, and the temperature allowed to vary) in order to have an estimation of the temperature and the mass of the cold dust.

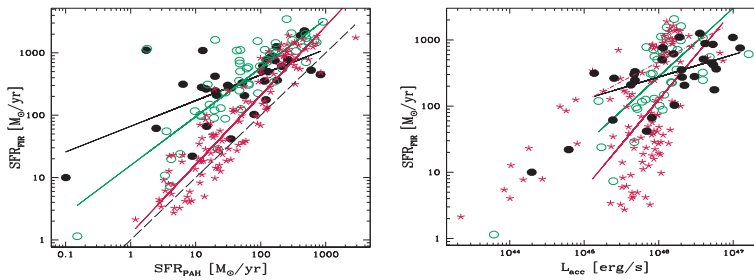


Figure 2. SFR_{FIR} versus SFR_{PAH} (left) and L_{acc} (right). Unobscured/obscured AGN- and starburst- dominated objects are represented in filled/open circles and stars, respectively.

3. Results and Discussion

We use a threshold value of the equivalent width of the PAH (measured on the IRS spectra), EW_{PAH} , equal to 0.2 (as found by Hernán-Caballero & Hatziminaoglou, 2011) to separate mid-IR AGN- ($\text{EW}_{\text{PAH}} < 0.2$) and starburst- ($\text{EW}_{\text{PAH}} > 0.2$) dominated objects. We use the PAH feature at $11.3 \mu\text{m}$ and that at $6.2 \mu\text{m}$ when the first was not available. Mid-IR AGN-dominated objects are further divided in obscured and unobscured, on the basis of the presence or no of the stellar component in the total best-fitting model. We compare various physical properties:

- SFR_{FIR} which is the SFR obtained applying the Kennicutt *et al.* (1998) prescription, $\text{SFR}_{\text{FIR}} = 4.5 \cdot 10^{-44} L_{\text{SB}}$, where L_{SB} (in erg/s) is the luminosity of the best fit starburst galaxy templates integrated between $8\text{--}1000 \mu\text{m}$;
- L_{acc} is the accretion luminosity of the best-fitting AGN torus models, representing the emission coming from the central accretion disk of AGN;
- SFR_{PAH} which is the SFR obtained using the correlations of Hernán-Caballero *et al.* (2009), $\text{SFR}_{\text{PAH}} = 1.4 \cdot 10^{-8} L_{\text{PAH}[6.2]}$ and $\text{SFR}_{\text{PAH}} = 1.52 \cdot 10^{-8} L_{\text{PAH}[11.3]}$ where $L_{\text{PAH}[6.2]}$ and $L_{\text{PAH}[11.3]}$ are the luminosities of the PAH features 6.2 and $11.3 \mu\text{m}$, respectively;
- the mass of the hot dust correspondent to the best-fitting torus model;
- the mass and the temperature of the cold dust estimated fitting the FIR data with a modified black body.

In Fig. 3 we report some of the main results of this work, extensively discussed Feltre *et al.* (2013). SFR_{FIR} correlates with SFR_{PAH} (left panel) as already found by previous authors (e.g. Schweitzer *et al.*, 2006; Netzer *et al.* 2007; Lutz *et al.*, 2008). Starburst-dominated objects (red stars) show the tighter and steeper correlation, very close to the 1:1 relation (dashed black line). The reason why SFR_{FIR} takes higher values with increasing SFR can be sought in the fact that the ratio between L_{PAH} and L_{SB} depends on this last. Indeed, we find a decrease of $L_{\text{PAH}}/L_{\text{SB}}$ with increasing L_{SB} . To investigate whether the presence of an AGN could affect the obscured SFR we compared the SFR_{FIR} as function of L_{acc} (right panel of Fig. 3) finding the first increasing with the AGN luminosity. Moreover, we find the ratio between L_{SB} and L_{acc} to decrease with L_{acc} .

Finally, we compared the properties of the hot (AGN heated) and cold (starburst heated) dust component. When fitting the modified black body we consider only objects with *Spitzer-MIPS* $160 \mu\text{m}$ in order to sample both sides of the cold dust emission peak. The mass of the hot dust and the cold dust mass do not show any evidence of a correlation (see left panel of Fig. 3). This reflects the fact that the two mechanisms occupy very different physical scales and, moreover, that gravitational effects that drive the star formation do not divert a fixed fraction of the gas towards the AGN centre while

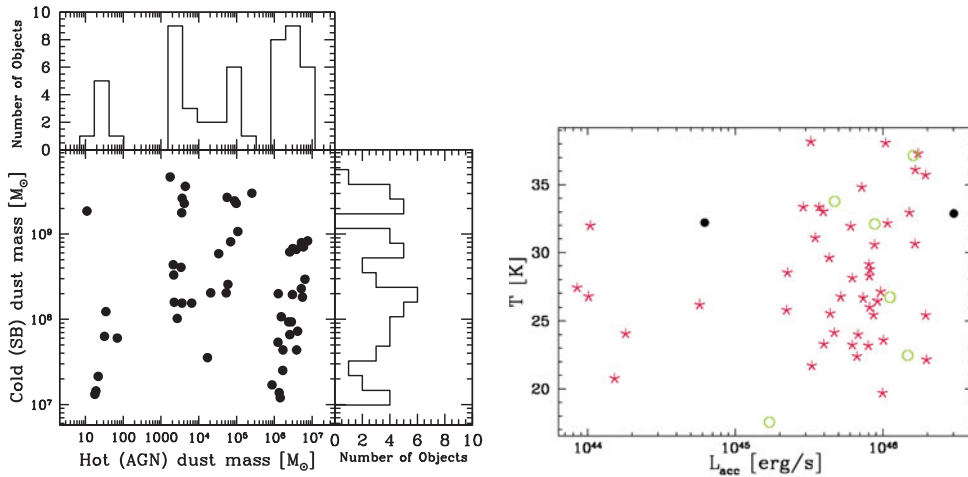


Figure 3. Cold (starburst-heated) versus hot (AGN-heated) dust masses (left) and cold dust temperature versus L_{acc} (right). AGN- and starburst- dominated objects are represented with circles and stars, respectively.

the starburst is ongoing. As can be seen in the right panel of Fig. 3 we also do not find any dependence of the temperature of the cold dust on L_{acc} .

To summarize, our findings do not provide evidence that the presence of an AGN can affect significantly the star formation processes of the host galaxies but rather than the two phenomena occur simultaneously over a wide range of luminosities. This is consistent with the expectation to see an average effect when considering large IR sample. Indeed, most models predict a very brief feedback phase, implying that a correlation between hot and cold dust properties is not expected to be seen, even with a feedback itself being very strong.

References

- Antonucci, R. R. J. & Miller, J. S. 1985, *ApJ*, 297, 621
 Urry, C. M. & Padovani, P. 1995, *PASP*, 107, 803
 Alexander, D. M., Bauer, F. E., Chapman, S. C., *et al.* 2005, *ApJ*, 632, 736
 Bertelli, G., Bressan, A., Chiosi, C., Fagotto, F., & Nasi, E. 1994, *AAPS*, 106, 275
 Bower R. G., Benson A. J., Malbon R., Helly J. C., Frenk C. S., Baugh C. M., Cole S., Lacey C. G. 2006, *MNRAS*, 370, 645
 Farrah, D., Afonso, J., Efstathiou, A., *et al.* 2003, *MNRAS*, 343, 585
 Feltre A., Hatziminaoglou E., Fritz J., Franceschini A. 2012, *MNRAS*, 426, 120
 Feltre, A., Hatziminaoglou, E., Hernán-Caballero, A., *et al.* 2013, *MNRAS*, 434, 2426
 Ferrarese L. & Merritt D. 2000, *ApJ*, 539, L9
 Fritz J., Franceschini A., Hatziminaoglou E. 2006, *MNRAS*, 366, 767
 Hernán-Caballero A. & Hatziminaoglou E. 2011, *MNRAS*, 414, 500
 Hernán-Caballero A., *et al.* 2009, *MNRAS*, 395, 1695
 Kennicutt, R. C., Jr. 1998, *ApJ*, 498, 541
 Lebouteiller V., Barry D. J., Spoon H. W. W., Sloan G. C., Houck J. R., Weedman D. W., 2011, *ApJS*, 196, 8
 Lutz, D., Sturm, E., Tacconi, L. J., *et al.* 2008, *ApJ*, 684, 853
 Netzer, H., Lutz, D., Schweitzer, M., *et al.* 2007, *ApJ*, 666, 806
 Oliver S., *et al.* 2012, *MNRAS*, 424, 1614
 Richards G. T., *et al.* 2006, *AJ*, 131, 2766
 Roseboom I. G., *et al.* 2010, *MNRAS*, 409, 48
 Schweitzer, M., Lutz, D., Sturm, E., *et al.* 2006, *ApJ*, 649, 79